Reversible and Continuous Latching Using a Carbon Internanotube Interface

Youngkee Eun, Jungwook Choi, Jae-Ik Lee, Hyungjoo Na, Dae-hyun Baek, Min-Ook Kim, and Jongbaeg Kim*

School of Mechanical Engineering, Yonsei University, 50 Yonsei-ro, Seodaemun-gu, Seoul 120-749, Republic of Korea

S Supporting Information

ABSTRACT: Mechanical multistability is greatly beneficial in micro-electromechanical systems because it offers multiple stable positioning of movable microstructures without a continuous energy supply. Although mechanical latching components based on multistability have been widely used in microsystems, their latching positions are inherently discrete and the number of stable positions is quite limited because of the lithographical minimum feature size limit of microstructures. We report a novel use of aligned carbon nanotube (CNT) arrays as latching elements in a movable micromechanical device. This CNT-array-based latching mechanism allows stable latching at multiple latching positions, together with reversible and bidirectional latching capabilities. The latching element with integrated CNTs on the sidewalls of microstructures can be adopted for diverse microelectromechanical systems that need precise positioning of movable structures without the necessity of continuous power consumption.

KEYWORDS: carbon nanotube, internanotube interface, adhesion, multistability
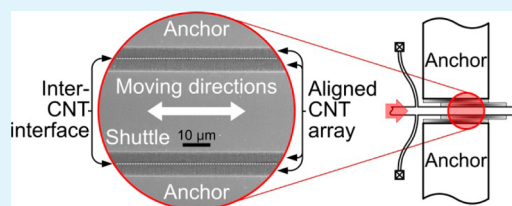
INTRODUCTION

Continuous power consumption throughout device operation is unavoidable in many microelectromechanical systems (MEMS). Even without any actuation or motion, energy needs to be continuously supplied just to maintain the displaced position or deformed configuration of the device.[1-4] In order to remove this state-maintaining power consumption, and thereby reduce the overall power consumption of the device, many approaches offering mechanical multistability have been developed. Mechanical multistability is extremely beneficial in microsystems, especially for variable or tunable electromechanical devices, because it offers multiple stable positioning of movable structures without the necessity of continuous energy supply. Mechanical latching elements have therefore been proposed and widely used in diverse MEMS applications, including accelerometers,[5] acceleration switches,[6] optical attenuators,[7] tunable capacitors,[8] and relays,[9] to ensure stable positioning of the movable parts without continuous power consumption. Most of these latching elements have predefined sawtooth-shaped microstructures for the latching mechanisms, as illustrated in Figure 1a. These devices gain multistability by using various rack-and-tooth-like mechanisms, as in macroscale machines. Accordingly, the latching precision strongly depends on the minimum feature size of the fabrication process, and consequently latching positions are inherently discrete, which results in a limited number of stable positions depending on the predefined shapes of the micro-structures.

Since the discovery of the role of van der Waals interactions in dry adhesion,[10,11] dry adhesives based on nanostructured materials have attracted much interest with a view to achieving

gecko-feet-mimicking bioinspired surfaces.[12,13] It has been discovered that a vertically aligned carbon nanotube (CNT) array generates a large adhesion force originating from van der Waals interactions and can be used as macroscale dry adhesives.[14-17] Various synthetic techniques for these highly ordered, vertically aligned CNT arrays have been intensively investigated.[18-21]

Despite the possibilities of the integration and use of CNT dry adhesives in microscale devices, this has not yet been explored in detail. In particular, the direct integration of CNT arrays in microstructures for practical applications of materials has not been extensively used. The integration of vertically aligned CNTs on the sidewall surfaces of single-crystal silicon microstructures has recently been introduced for some applications, including micromechanical switches,[22] contact-time-enhanced acceleration switches,[23] interfacial materials that offer intimate contact for displacement sensors,[24] and silicon plastic processing.[25] Because of their exceptional elastic modulus,[26] strength,[27] resilience,[28] compressibility,[29] wear and fatigue resistances,[19] and electrical and thermal conductivities,[30,31] CNT-integrated devices show enhanced performances along with reliable long-term operation, which is difficult to achieve using conventional approaches.

On the basis of previous reports on the integration of CNT arrays into microelectromechanical devices using a mechanically constrained synthetic method that creates internanotube contact interfaces,[22-25,32] we developed a continuously latching
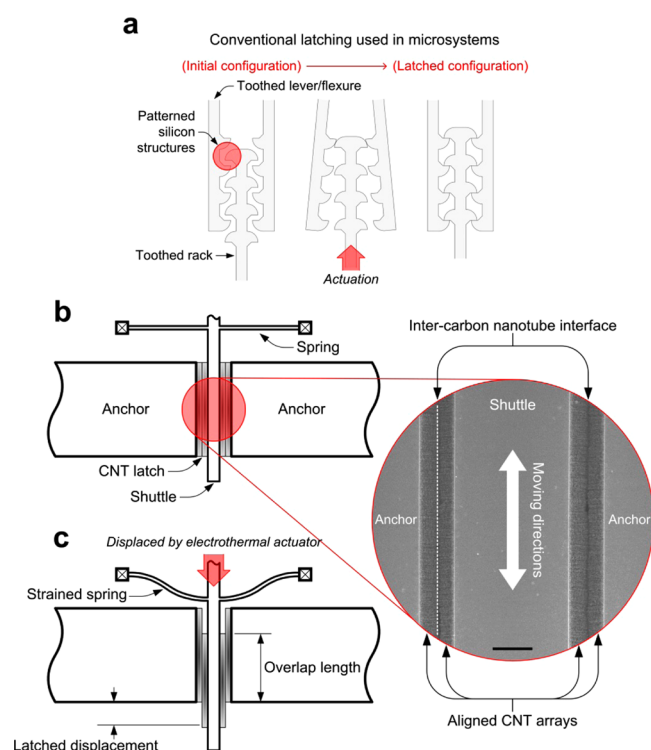
Figure 1. Comparison between conventional latching in microsystems and CNT-array-based latching. (a) Conventional sawtooth-shaped microstructure-based latching mechanism used in microsystems. (b) Initial configuration of the CNT-array-based latching element. Aligned CNT arrays are synthesized on the sidewall surfaces of silicon microstructures. Trenches between the shuttle and anchors are filled with aligned CNT arrays, forming internanotube contact interfaces (the scale bar in the inset image is 10 μm). (c) Latched state configuration of the shuttle. The shuttle is displaced to a desired position by an external actuation force, and the CNT latch holds the shuttle against the elastic restoring force of the strained springs.

micromechanical element that provides numerous stable positions, using CNT arrays integrated on the sidewalls of movable and stationary microstructures. The CNT array is directly synthesized inside the gap between the movable shuttle and two fixed anchors, one of which is placed on each side of the shuttle. The CNT latch element sustains the elastic restoring force of the strained springs and fixes the shuttle at the desired position. The demonstrated latching shuttle with CNT arrays shows stable, reversible, and bidirectional latching capabilities. Furthermore, the CNT-based latching element effectively delivers the ability to hold the movable structure in multiple stable positions without the necessity of continuous power consumption.

EXPERIMENTAL METHODS

Fabrication of a CNT-Based Latching Element. For the silicon microstructures, photoresist and aluminum etch masks were patterned on the front and back, respectively, of silicon-on-insulator (SOI) wafers, using photolithography. Deep reactive ion etching was then performed on both the device silicon layer and the substrate, in order to define silicon microstructures on the device layer and the backside holes. After deep etching, both of the remaining etch mask layers were removed and the movable structures were released by etching the buried oxide layer using a hydrofluoric acid vapor.[39] After release of the movable structures defined on the device layer, a 5-nm-thick iron catalyst film was deposited by electron-beam evaporation. The catalyst layer was patterned either from the front using a shadow mask or from

the back of the wafer through the predefined backside holes, depending on the device design. The CNT arrays were then synthesized on only the iron-covered area by catalytic thermal chemical vapor deposition. The substrate was heated to 700 °C in a furnace with a nitrogen atmosphere. The atmospheric gas was then converted to ammonia (100 sccm) for the pretreatment.[40] After 30 min of ammonia flow, acetylene (50 sccm) was introduced in order to activate CNT growth; growth was performed for 15 min.

RESULTS AND DISCUSSION

For formation of the CNT-array-based latching element, narrow gaps are defined on both sides of a movable shuttle by conventional silicon-processing techniques, and then vertically aligned CNT arrays are synthesized on the sidewall surfaces of the gaps, as shown in Figure 1b. After CNT growth, the gaps between the shuttle and the two anchors are filled with highly ordered CNT arrays, forming an internanotube contact interface. When the shuttle is displaced to a desired position by an external actuation force (Figure 1c), it is latched by the CNTs and holds that position even after the actuation force is removed. Two electrothermal actuators[33,34] for pushing the shuttle are cofabricated, one at each end of the shuttle, for bidirectional motion generation. In the latched state, the elastic restoring force of the mechanical spring is smaller than the internanotube adhesion force. In this way, unlike previous latching mechanisms in micromechanical devices, stable latching at any desired position within a latchable range is achieved by simple CNT integration, without the necessity for predefined microstructures such as sawtooth, ratchet, or additional flexure mechanisms. This approach does not require high-resolution patterning to obtain the small and sharp sawtooth-shaped latching structures used in conventional latching mechanisms (Figure 1a or its variations) and allows precise and continuous latching with an infinite number of stable positions. As long as the CNTs on the sidewall surfaces of the shuttle are engaged with the facing set of CNTs on the sidewall surfaces of the anchor and unless the elastic restoring force exceeds the adhesive force exerted from CNT−CNT contacts, the shuttle can be further displaced to be latched at another position or pushed in the opposite direction to be reversed to the initial position.

Compared with previous CNT-based dry adhesives[14−17] and interlocking fiber-based dry adhesives,[35,36] where the micro/nanostructures are forced to overlap each other by preloading, the CNT latch does not require preloading steps after fabrication. So, unlike adhered or locked configurations, in which large portions of the length overlap each other, only a small part of the internanotube interface is in contact for the CNT latch. This slight internanotube interface contact provides a moderate resistance in the sliding direction, so that the shuttle is held in the latched position against the elastic restoring force of the deformed springs.

The CNT-array-based latching mechanism was fabricated on a heavily doped SOI wafer. The CNT arrays were only integrated in the single-crystal silicon microstructures by direct synthesis at desired locations. [Details are presented in the Experimental Methods section, and the full fabrication process is illustrated in the Supporting Information (SI), Figure S1.] The diameters of the produced CNTs were measured using high-resolution scanning electron microscopy (SEM; JEOL-6701F). The average diameter of 20 CNTs was 11.5 nm, and the standard deviation was 2.2 nm. The fabricated CNT-array-based latch and silicon structures were determined using SEM

(Figure 2a). Highly ordered CNT arrays were synthesized on both sides of the shuttle and completely filled the gaps between
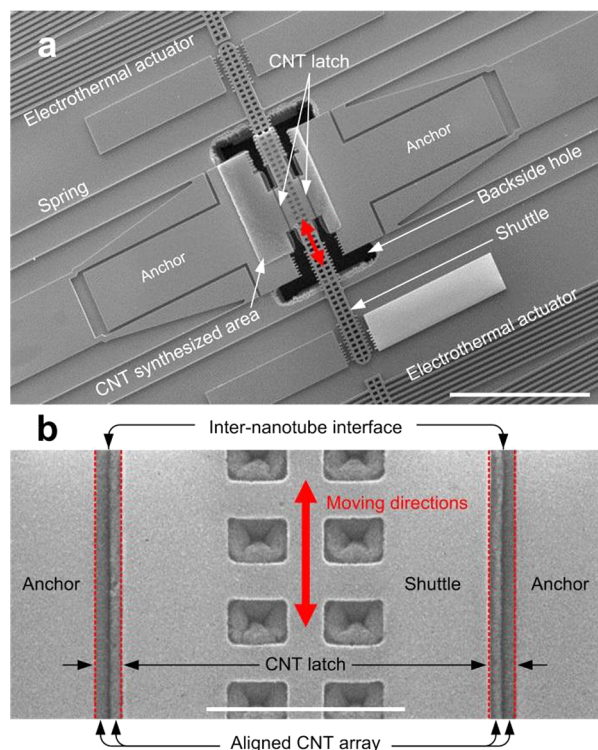

Figure 2. SEM images of fabricated CNT latch and silicon microstructures. (a) Overview of the CNT-array-based latching element and electrothermal actuators (the scale bar is 500 μm). (b) Enlarged image of the CNT latch and shuttle. The aligned CNT arrays integrated between the shuttle and the anchors form internanotube contact interfaces along the center line of the trench gap (the scale bar is 50 μm).

the shuttle and the two anchors, forming a CNT−CNT contact interface at the center line of each gap (Figure 2b). This inter-CNT interface is maintained without the interfaces penetrating each other, even with an increased synthesis time, because of the strong van der Waals interactions between neighboring CNTs within the CNT array.

Latching tests were performed and monitored under an optical microscope. The CNT arrays are highly antireflective and appear black under optical microscopic observation[37] (Figure S2 in the SI). The device was unpackaged and exposed to the atmospheric environment throughout the tests. In the initial state, there is no elastic restoring force from the springs. Then, by driving one of the two thermal actuators, one of which is placed at each end of the shuttle, the shuttle is displaced to a desired position. The shuttle and the thermal actuators are designed to be initially separated, and the shuttle is only supported by the springs. Because the CNTs on the sidewalls of the anchors hold the CNTs on the shuttle, the shuttle is latched against the elastic restoring force of the springs (Figure S3a in the SI). Without the integrated CNT latching element, the shuttle returns to its initial position as soon as the driving force is removed, as a result of elastic recovery of the supporting springs. In contrast, with the CNT latch, the shuttle remains at its latched position even after the driving force is removed (see Movie S1 in the SI). In the design of the CNT latch shown in Figure 1c, as the shuttle

displacement increases, the overlap length between CNTs decreases, while the elastic restoring force of the springs increases. Because the smaller overlap length results in a smaller latching force, there is a maximum latchable displacement of the shuttle. The experimentally measured maximum latchable displacement is 28 μm, where the spring force equals the adhesion force of the CNTs. This latchable range can be adjusted, depending on the application, by appropriately designing the spring stiffness and the overlap length between CNTs. On the basis of the force balance, the corresponding latching force per unit area is estimated to be 15 N/cm^2. (Detailed calculations are presented in the text and Figure S3b in the SI.)

Compared with conventional sawtooth-shaped discretely latching microstructures, CNT latches can be latched at any desired positions within the maximum latchable displacement because of the random locational distribution and large number of CNTs on the sidewall surfaces. Ideally, by taking advantage of the number and size of the CNTs, there can be a very large number of stable positions within the latching range, enabling continuous latching. So, when the CNT arrays are sufficiently dense, high-resolution latching can be achieved. We monitored the latching positions while driving the electrothermal actuators with a gradually increasing sinusoidal voltage input (Figure 3). The dynamic displacement measurement was performed by discrete Fourier analysis of charge-coupled-device camera images; this method was introduced by Yamahata et al.[38] The resultant latching behaviors for 47 consecutive stable latching positions were determined and are presented in Figure 3a. The white columns represent the latched displacement of each latching, and the red columns represent the incremental displacements with respect to the latching steps. The average incremental displacement was about 600 nm.

A closer look in the time domain shows that there is a significant amount of backlash, i.e., loss of motion, before firm latching (Figure 3b). The magnitude of the backlash with respect to the latch steps is shown as the gray column on top of the latch displacement column (Figure 3a). The backlash displacement tends to increase as the latch steps increase, and it ranges between 82 nm and 1.5 μm. The backlash generation could be explained by elastic deformation of the CNTs due to the restoring force of the springs (see the text and Figure S4 in the SI).

Reversible and bidirectional latching capability is another advantage of the proposed CNT-array-based latching element. Using the two electrothermal actuators, the shuttle can be displaced in both the forward and backward directions, and the latching function is successfully demonstrated during this bidirectional motion (see Movie S1 in the SI). This is not possible using conventional microlatching elements, where the reverse motion is not allowed once the structure is latched.

For practical application of the latching element in micromechanical devices, it is essential to verify its reliability. Stability and repeatability tests were performed in order to verify the latching reliability. In the static stability tests, where the elastic restoring force of the strained springs acted as a constant load against the CNT latch, the latched displacement was monitored over time. No change in the latched position was observed for over 48 h. This result indicates that the latched configuration of the device is in a balanced state and is maintained unless there is any external disturbance. Repeatability tests, in which the shuttle was latched at a displaced position and reversed to the original position repeatedly, were
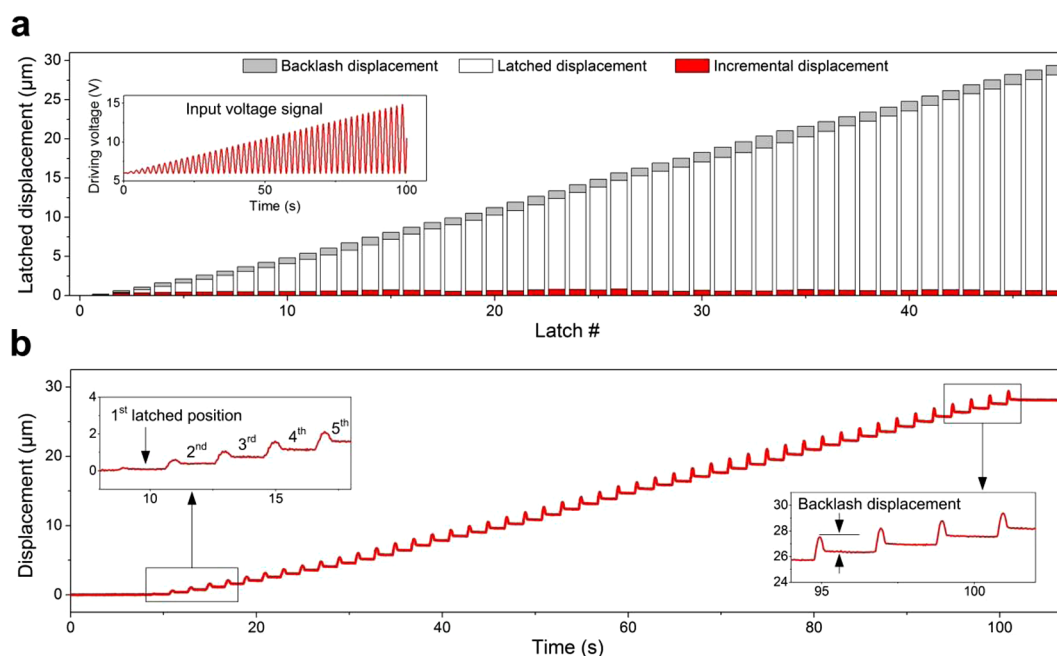
Figure 3. Consecutive stable latching of the CNT-array-based latching element. (a) Latched displacement with respect to latching steps while driving an electrothermal actuator with gradually increasing sinusoidal voltage (inset). White columns represent latched displacement, red columns represent incremental displacement, and gray columns represent backlash displacement with respect to latching steps. (b) Displacement of the shuttle in the time domain.

then performed by actuating the two thermal actuators consecutively for over 7200 cycles. For the first 3600 cycles, a 6% deviation in latched displacement was observed, and for the next 3600 cycles, no deviation or failure was observed (Figure 4). The device was inspected using SEM to identify any distortions of the CNT arrays after the tests; however, it was hard to tell if there was any significant distortion or morphological changes. The current flowing through two sets of internanotube interfaces was also monitored during the repeatability tests. In the early stage of the repeatability test, because the temperature coefficient of resistance of the CNT
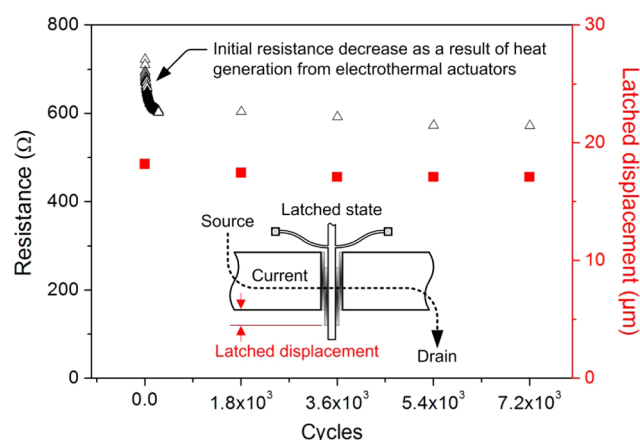
array is negative in our case,[22] the electrical resistance started to decrease as a result of the heat generated by the electrothermal actuators. After temperature stabilization, the resistance also stabilized and showed only minor changes over repeated cycles. The resistance was recovered when the actuators were turned off because the initial resistance decrease is mainly the result of the temperature increase caused by the electrothermal actuators.

Additionally, to verify the latching robustness, vibration endurance tests were performed by applying an external acceleration to the device. The acceleration was generated by a vibration exciter and measured using a reference accelerometer. The direction of the acceleration was aligned to be parallel to the movable direction of the shuttle (Figure S5 in the SI). Up to 30 g of external excitation, there was no observable deviation in the latched position. The corresponding force exerted by the input acceleration was estimated to be around 2 μN at 30 g, based on the mass of the shuttle. The estimated sustainable acceleration per unit area of internanotube contact interface was 2.2 g/μm^2.

CONCLUSIONS

In conclusion, we have developed a novel latching element that provides continuously adjustable latching positions with reversible and bidirectional latching capabilities, using integrated CNT arrays. Stable consecutive latching within a large latching range was achieved, and the repeatability and reliability were experimentally verified through thousands of cyclic latching tests. By adoption of facile integration methods, in which the CNTs are grown directly on the fully fabricated microstructures, the CNT latch can be used as an essential element in diverse MEMS applications where the precise positioning of the movable structures and holding of the displaced position are required, without the necessity of power consumption.

Figure 4. Long-term latching reliability of the CNT latch at atmospheric pressure. Cyclic loading is performed by repeating latching and reversing between two positions, using two thermal actuators. The latched displacement and the current flowing through the CNT arrays are monitored simultaneously. The resistance decrease in the early stage of the reliability test is caused by heat generation from the electrothermal actuators and the negative temperature coefficient of resistance of the CNT arrays of our device.[22]

■ ASSOCIATED CONTENT

Ⓢ Supporting Information

Additional text, movie, and figures, including a detailed fabrication process, an optical microscope image of the fabricated CNT latch, the force−displacement relationship, the backlash behavior of the CNT latch, a schematic diagram of the acceleration test setup, and a movie of the operation of the CNT-array-based latching element. This material is available free of charge via the Internet at http://pubs.acs.org.

■ AUTHOR INFORMATION

Corresponding Author
*E-mail: kimjb@yonsei.ac.kr.

Notes
The authors declare no competing financial interest.

■ ACKNOWLEDGMENTS

■ REFERENCES

(1) Toshiyoshi, H.; Fujita, H. *J. Microelectromech. Syst.* **1996**, *5*, 231−237.

(2) Zhu, W. M.; Liu, A. Q.; Bourouina, T.; Tsai, D. P.; Teng, J. H.; Zhang, X. H.; Lo, G. Q.; Kwong, D. L.; Zheludev, N. I. *Nat. Commun.* **2012**, *3*, 1274.

(3) Xiao, Z.; Peng, W.; Wolffenbuttel, R. F.; Farmer, K. R. *Sens. Actuators, A* **2003**, *104*, 299−305.

(4) Nguyen, H. D.; Hah, D. Y.; Patterson, P. R. R.; Chao, R. M.; Piyawattanametha, W.; Lau, E. K. K.; Wu, M. C. C. *J. Microelectromech. Syst.* **2004**, *13*, 406−413.

(5) Ciarlo, D. R. *J. Micromech. Microeng.* **1992**, *2*, 10−13.

(6) Sun, X.-Q.; Zhou, S.; Carr, W. N. *Proceedings of the 9th IEEE International Conference on Solid-State Sensor and Actuators*, Chicago, IL, 1997; IEEE: New York, 1997, pp 1189−1192.

(7) Syms, R. R. A.; Zou, H.; Boyle, P. *J. Microelectromech. Syst.* **2005**, *14*, 529−538.

(8) Reinke, J.; Fedder, G. K.; Mukherjee, T. *J. Microelectromech. Syst.* **2010**, *19*, 1105−1115.

(9) Sun, X.-Q.; Farmer, K. R.; Carr, W. N. *Proceedings of the 11th IEEE International Conference on Micro Electro Mechanical Systems*, Heidelberg, Germany, 1998; IEEE: New York, 1998; pp 154−159.

(10) Autumn, K.; Liang, Y. A.; Hsieh, S. T.; Zesch, W.; Chan, W. P.; Kenny, T. W.; Fearing, R.; Full, R. J. *Nature* **2000**, *405*, 681−685.

(11) Autumn, K.; Sitti, M.; Liang, Y. A.; Peattie, A. M.; Hansen, W. R.; Sponberg, S.; Kenny, T. W.; Fearing, R.; Israelachvili, J. N.; Full, R. J. *Proc. Natl. Acad. Sci. U. S. A.* **2002**, *99*, 12252−12256.

(12) Jeong, H.-E.; Suh, K. Y. *Nano Today* **2009**, *4*, 335−346.

(13) Sameoto, D.; Menon, C. *Smart Mater. Struct.* **2010**, *19*, 103001.

(14) Yurdumakan, B.; Raravikar, N. R.; Ajayan, P. M.; Dhinojwala, A. *Chem. Commun.* **2005**, 3799−3801.

(15) Zhao, Y.; Tong, T.; Delzeit, L.; Kashani, A.; Meyyappan, M.; Majumdar, A. *J. Vac. Sci. Technol., B: Nanotechnol. Microelectron.: Mater., Process., Meas., Phenom.* **2006**, *24*, 331.

(16) Ge, L.; Sethi, S.; Ci, L.; Ajayan, P. M.; Dhinojwala, A. *Proc. Natl. Acad. Sci. U. S. A.* **2007**, *104*, 10792−10795.

(17) Qu, L.; Dai, L. M.; Stone, M.; Xia, Z. H.; Wang, Z. L. *Science* **2008**, *322*, 238−242.

(18) Cao, A.; Veedu, V. P.; Li, X. S.; Yao, Z. L.; Ghasemi-Nejhad, M. N.; Ajayan, P. M. *Nat. Mater.* **2005**, *4*, 540−545.

(19) Toth, G.; Mäklin, J.; Halonen, N.; Palosaari, J.; Juuti, J.; Jantunen, H.; Kordas, K.; Sawyer, W. G.; Vajtai, R.; Ajayan, P. M.; Maklin, J. *Adv. Mater.* **2009**, *21*, 2054−2058.

(20) Hart, A. J.; Slocum, A. H. *Nano Lett.* **2006**, *6*, 1254−1260.

(21) Meshot, E. R.; Hart, A. J. *Appl. Phys. Lett.* **2008**, *92*, 113107.

(22) Choi, J.; Lee, J.-I.; Eun, Y.; Kim, M.-O.; Kim, J. *Adv. Mater.* **2011**, *23*, 2231−2236.

(23) Lee, J.; Song, Y.; Jung, H.; Choi, J.; Eun, Y.; Kim, J. *IEEE Trans. Ind. Electron.* **2012**, *59*, 4914−4920.

(24) Lee, J.-I.; Choi, J.; Lee, K.; Jeong, B.; Kim, J. *Proceedings of the IEEE 23rd International Conference on Micro Electro Mechanical Systtems*, Wanchai, Hong Kong, 2010; IEEE: New York, 2010; pp 627−630.

(25) Eun, Y.; Lee, J.-I.; Choi, J.; Song, Y.; Kim, J. *Adv. Mater.* **2011**, *23*, 4285−4289.

(26) Treacy, M. M. J.; Ebbesen, T. W.; Gibson, J. M. *Nature* **1996**, *381*, 678−680.

(27) Yu, M.-F.; Lourie, O.; Dyer, M. J.; Moloni, K.; Kelly, T. F.; Ruoff, R. S.; Yu, M.-F. *Science* **2000**, *287*, 637−640.

(28) Falvo, M. R.; Clary, G. J.; Taylor, R. M.; Chi, V.; Brooks, F. P.; Washburn, S.; Superfine, R. *Nature* **1997**, *389*, 582−584.

(29) Cao, A.; Dickrell, P. L.; Sawyer, W. G.; Ghasemi-Nejhad, M. N.; Ajayan, P. M. *Science* **2005**, *310*, 1307−1310.

(30) Ebbesen, T. W.; Lezec, H. J.; Hiura, H.; Bennett, J. W.; Ghaemi, H. F.; Thio, T. *Nature* **1996**, *382*, 54−56.

(31) Kim, P.; Shi, L.; Majumdar, A.; McEuen, P. L. *Phys. Rev. Lett.* **2001**, *87*, 19−22.

(32) Eun, Y.; Choi, J.; Na, H.; Baek, D.; Kim, M.-O.; Lee, J.; Kim, J. *Proceedings of the 25th IEEE International Conference on Micro Electro Mechanical Systems*, Paris, France, 2012; IEEE: New York, 2012; pp 80−83.

(33) Que, L.; Park, J.-S.; Gianchandani, Y. B. *J. Microelectromech. Syst.* **2001**, *10*, 247−254.

(34) Lott, C. D.; McLain, T. W.; Harb, J. N.; Howell, L. L. *Sens. Actuators, A* **2002**, *101*, 239−250.

(35) Pang, C.; Kim, T.; Bae, W. G.; Kang, D.; Kim, S. M.; Suh, K.-Y. *Adv. Mater.* **2012**, *24*, 475−479.

(36) Ko, H.; Zhang, Z.; Ho, J. C.; Takei, K.; Kapadia, R.; Chueh, Y.; Cao, W.; Cruden, B. A.; Javey, A. *Small* **2010**, *6*, 22−26.

(37) Yang, Z.-P.; Ci, L.; Bur, J. A; Lin, S.-Y.; Ajayan, P. M. *Nano Lett.* **2008**, *8*, 446−451.

(38) Yamahata, C.; Sarajlic, E.; Krijnen, G. J. M.; Gijs, M. A. M. *J. Microelectromech. Syst.* **2010**, *19*, 1273−1275.

(39) Fukuta, Y.; Fujita, H.; Toshiyoshi, H. *Jpn. J. Appl. Phys.* **2003**, *42*, 3690−3694.

(40) Lee, D. H.; Lee, W. J.; Kim, S. O. *Nano Lett.* **2009**, *9*, 1427−1432.